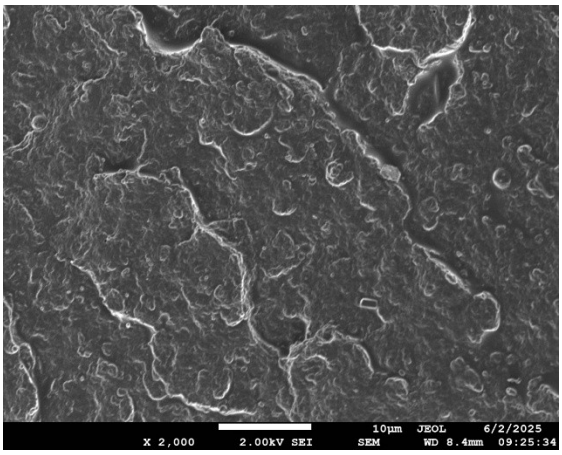

(a) PLA + 0.5 wt% Ag (mixing)

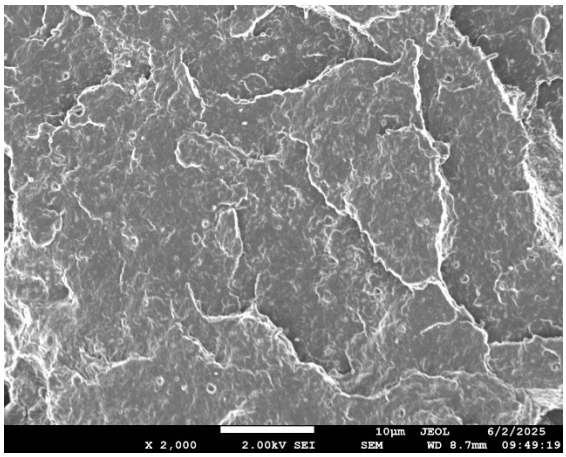

(b) PLA + 1 wt% Ag (mixing)

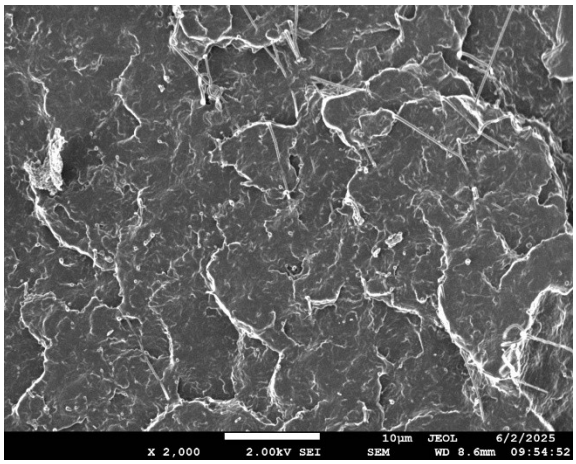

(c) PLA + 0.5 wt% Cu (mixing)

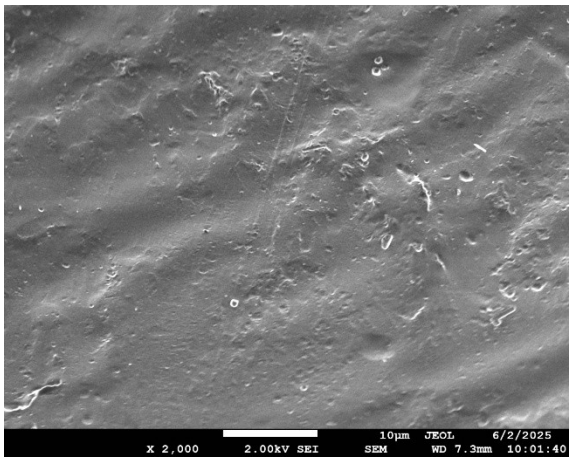

(d) PLA + 1 wt% Cu (mixing)

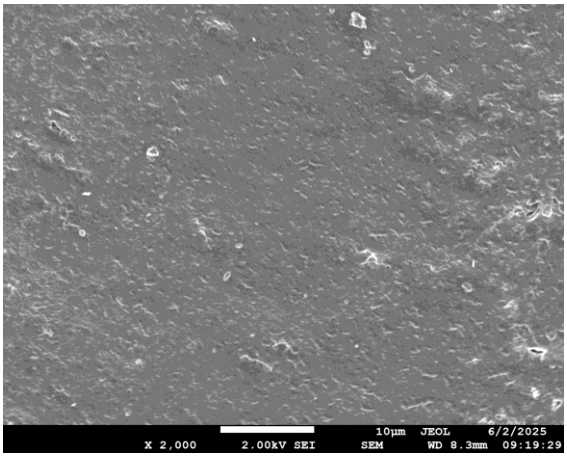

(e) PLA + 0.5 wt% Ag (in situ ROP)

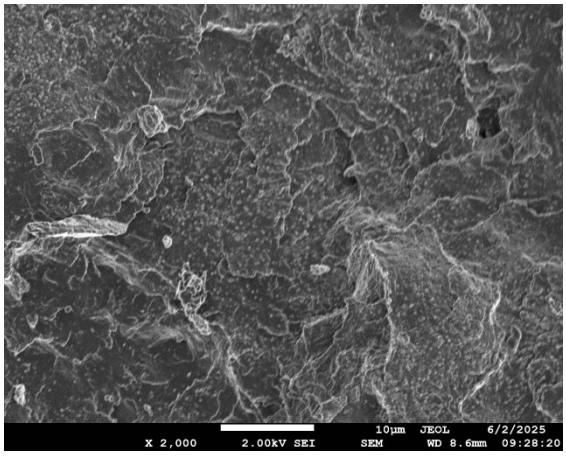

(f) PLA + 1 wt% Ag (in situ ROP)

Figure S1. SEM micrographs of all PLA-based PNCs, prepared by both (a-d) mixing and (e,f) in situ ROP captured at the cross-section. The scale bars correspond to 10 μm.

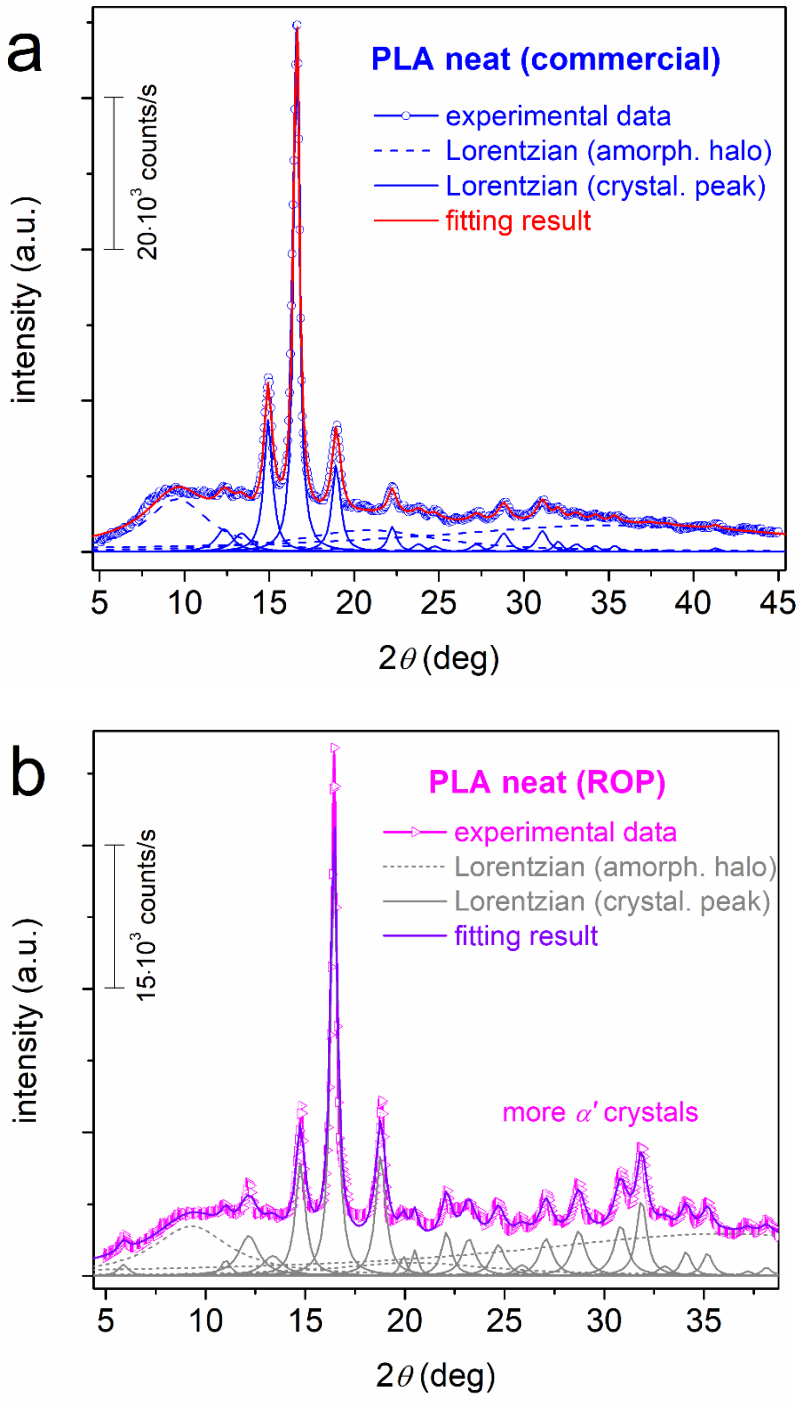

Figure S2. Examples of analysis of the XRD spectra for the neat PLA samples, namely, (a) the commercial and (b) the one prepared by ring opening polymerization, ROP, of l-lactide.

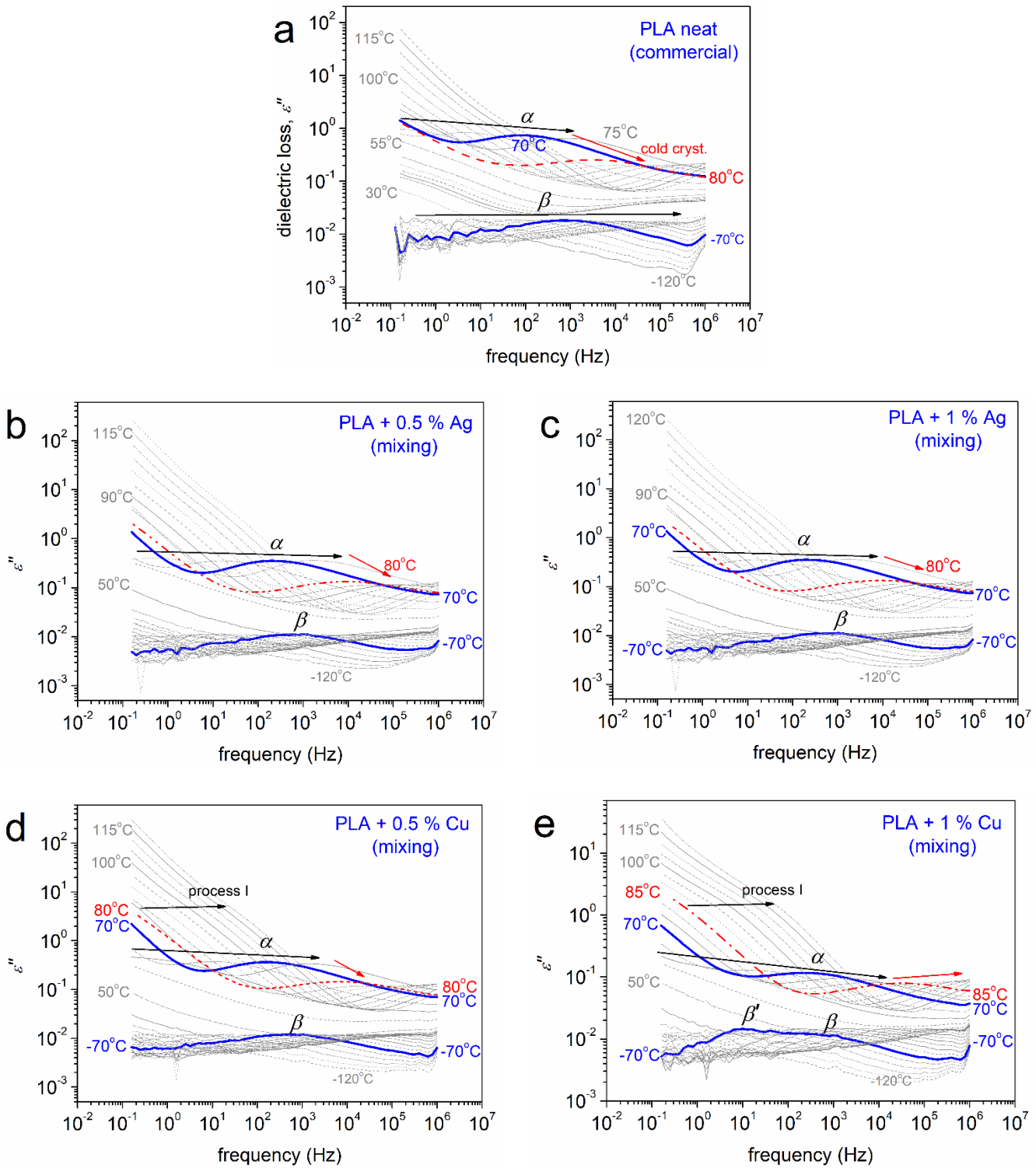

Figure S3. Raw BDS data for commercial (a) PLA and (b-e) the PLA-based PNCs prepared by mixing, in the form of isothermal $\varepsilon''(f)$ curves. The marked isothermals at selected temperatures show the main relaxation processes (β, β' and α).

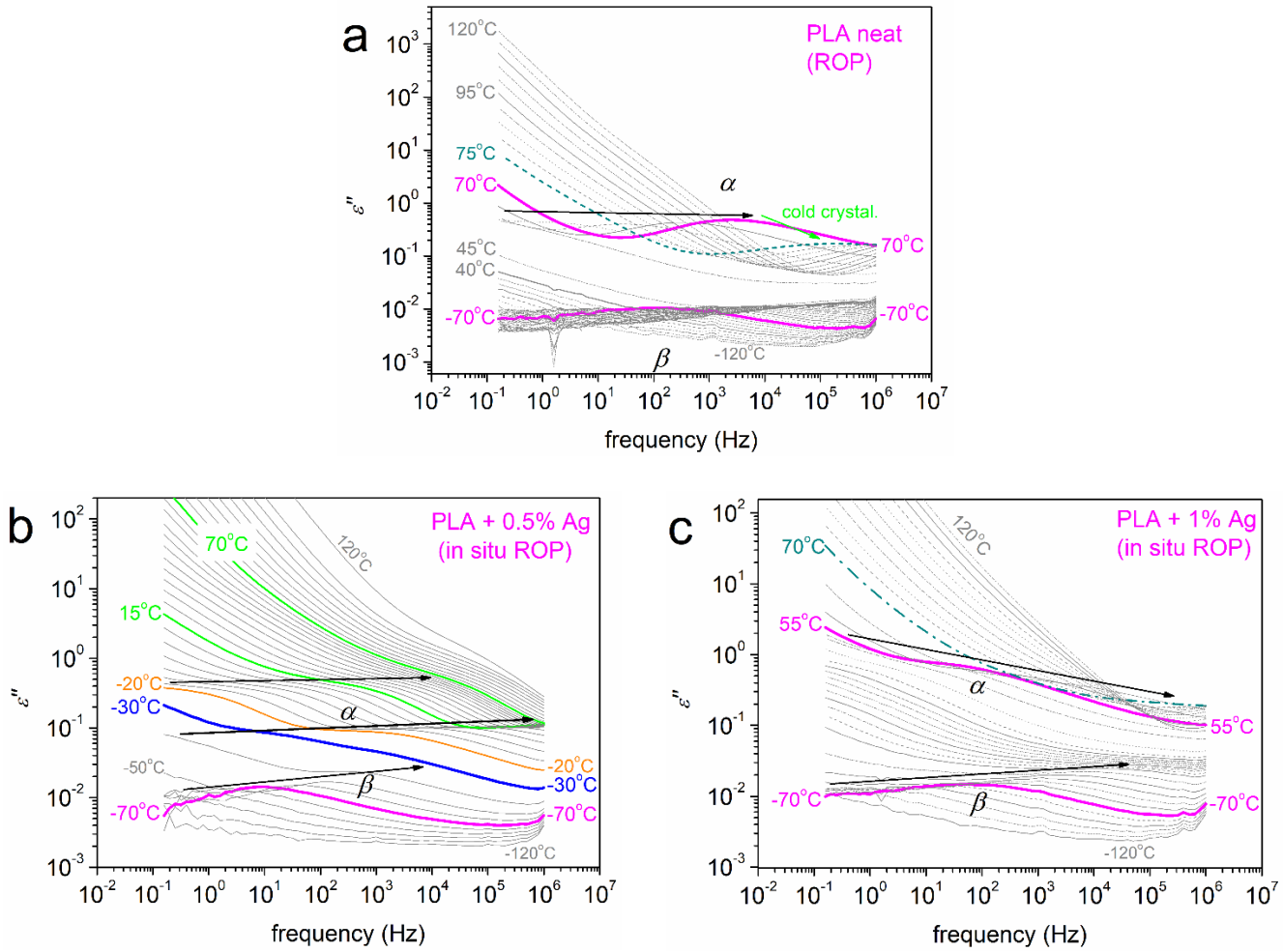

Figure S4. The raw BDS data for (a) neat PLA prepared by ROP and (b-e) the PLA-based PNCs prepared by the in-situ ROP of lactide. At the selected temperatures, the marked isothermal $\varepsilon''(f)$ curves present the main relaxation processes (β, α) as well-formed peaks.

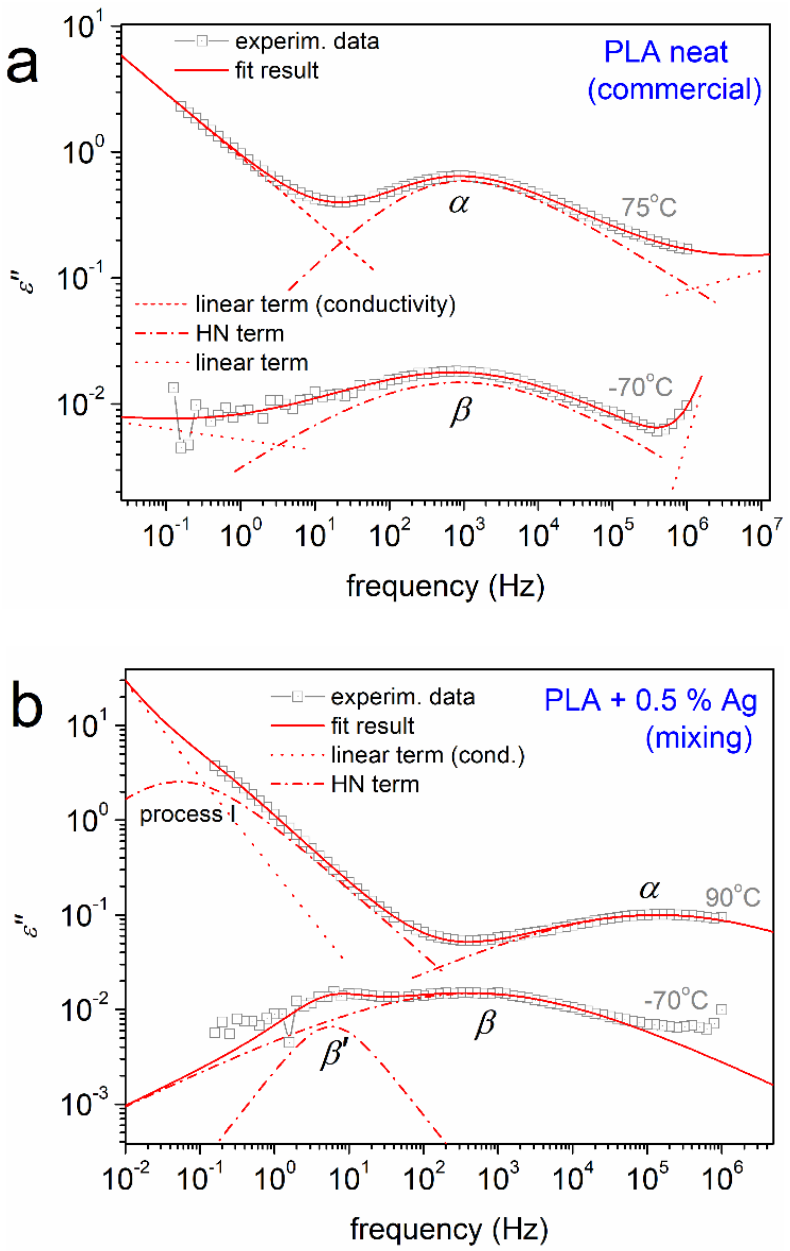

Figure S5. Examples of analysis of the complex $\varepsilon''(f)$ isothermals in terms of model mathematical functions, i.e., Havriliak-Negami (HN) and linear terms, for the selected samples and temperatures, being indicated on the plots.